

# **Multigrid Method in Modeling Contact between Liner Finish and Piston Ring Pack in Internal Combustion Engines**

**Qing Zhao**

**Sloan Automotive Lab, Massachusetts Institute of Technology**

**Abstract:** A numerical simulation based on multigrid method is created to model contact between liner finish and piston ring pack in internal combustion engines. 3D measured surface of liner finish given by confocal microscope serves as an input in this model. It applies multigrid method to obtain fast convergence of the problem. This model predicts contact pressure on liner finish due to contact with ring surface at certain clearance height, and corresponding deformed liner surface. Contact between liner finish and piston ring pack in internal combustion engines is very important in understanding friction between them and finding potential solutions to reduce oil consumption in automotive industry.

## **1. Introduction**

When decreasing of fossil fuel supplies and air pollution are two major society problems in the 21<sup>st</sup> century, rapid growth of internal combustion (IC) engines serves as a main contributor of these two problems. The challenge of energy demand and environmental protection can be alleviated by increasing the engine's efficiency and reducing its CO<sub>2</sub> emissions. These are the two demanding goals for the whole automotive industry. Among total consumed energy in a typical diesel automotive, mechanical friction loss accounts for approximately 10% of the total fuel energy, and of which around 20% is dissipated into friction between piston rings and liner finish [1]. As a result, there is still a space for automotive industry to increase energy efficiency by reducing piston ring pack friction.

Asperity contact between liner finish and rings can occur due to a combination of limited oil supply and low piston sliding speed at top dead center (TDC) and bottom dead center (BDC) of the stroke among piston ring pack friction. Asperity contact occurs in a boundary lubrication regime, when asperities carry the entire ring load, and in a mixed lubrication regime, when the ring load is shared by asperity contact and hydrodynamic pressure. Friction due to asperity contact has been identified as an important contributor to total ring pack friction [2]. And thus, a method to predict contact friction between piston ring pack and liner finish is necessary.

In a combustion chamber of an internal combustion engine, a piston ring is a split ring that fits into a groove on the outer diameter of a piston and the main functions of piston rings are sealing the combustion chamber so that there is no transfer of gases and oil from the combustion chamber to the crank case and regulating engine oil consumption [3]. The piston ring pack consists of three different rings (from top to bottom): top ring (compression ring), second ring (scraper ring) and oil control ring (OCR), as illustrated in Figure 1. Due to manufacturing process, the surface of piston rings can be modeled as purely smooth surface.

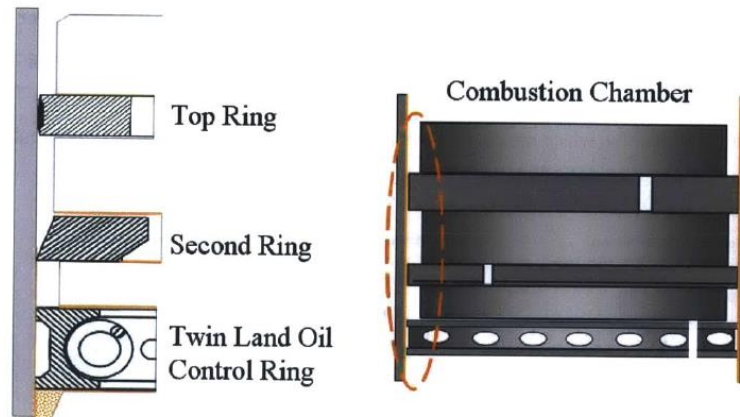


**Figure 1: Position of Piston Ring Pack in Combustion Chamber of an Internal Combustion Engine**

To guarantee reproducibility with efficient productivity in mass production, cylinder liners of internal combustion engines are finished using an interrupted multi-stage honing process and it generates plateau and valley area on it. Surface of liner finish cannot be modeled as smooth surface and its real surface geometry can be measured through optical microscope or stylus measurement technique. Figure 2 shows a small patch of measured liner finish (size: 0.185 mm by 0.185 mm) and its resolution is 0.37 micro in both axial and circumferential directions.

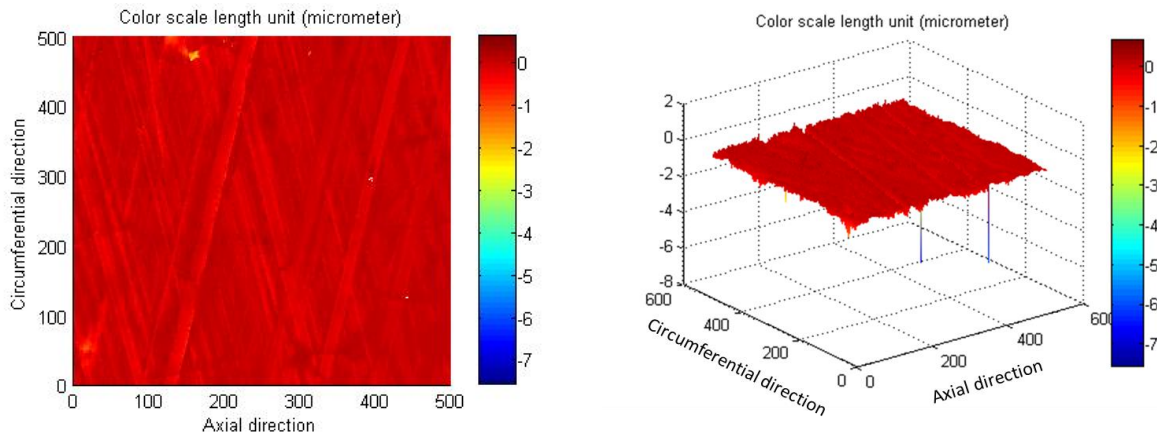


**Figure 2: Sample Liner Geometry Profile in 2D and 3D View**

## 2. Problem Description

Modeling contact pressure between liner finish and piston ring pack at certain clearance height  $h_0$  is the most important challenge in predicting contact friction between them. In real situation, the assumption that ring surface is purely smooth surface can be made due to the fact that surface roughness of piston ring is negligible when compared with that of liner finish. The purpose of this project is to establish a numerical method to solve contact pressure between a measured surface and a purely smooth surface at clearance height  $h_0$  between them, as illustrated in Figure 3. The rough surface is represented by a matrix reflecting the height at each spot. In this project, it is constrained to elastic deformation between the two surfaces.

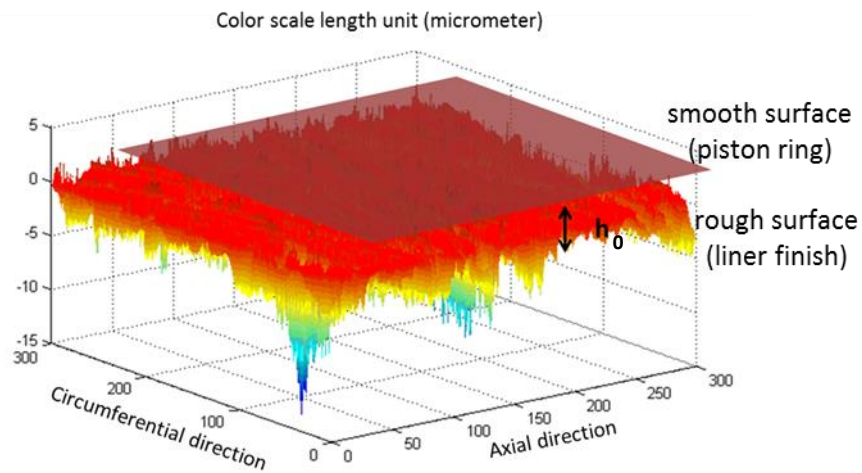


**Figure 3: Contact between a Rough Surface (Liner Finish) and a Smooth Surface (Piston Ring Surface)**

If height of one spot  $l(x, y)$  on rough surface is larger than clearance height  $h_0$ , it will deform and generate pressure  $p(x, y)$  between them due to compression. In order to approximate contact pressure, Lubrecht derives an equation that relates deformation of a spot  $w(x, y)$  to pressure distribution on the whole surface [4]:

$$w(x, y) = \frac{2}{\pi E'} \int_{-\infty}^{+\infty} \int_{-\infty}^{+\infty} \frac{p(x', y') dx' dy'}{\sqrt{(x - x')^2 + (y - y')^2}}$$

where

$$\frac{2}{E'} = \frac{1 - \nu_1^2}{E_1} + \frac{1 - \nu_2^2}{E_2}$$

and  $\nu_1$  and  $\nu_2$  represent Poisson ratio of rough surface and smooth surface.  $E_1$  and  $E_2$  are elastic moduli of them respectively.

Defining gap between rough surface and smooth surface at each spot as  $h(x, y)$ , finally gives it as:

$$h(x, y) = h_0 - l(x, y) + \frac{2}{\pi E'} \int_{-\infty}^{+\infty} \int_{-\infty}^{+\infty} \frac{p(x', y') dx' dy'}{\sqrt{(x - x')^2 + (y - y')^2}}$$

When two spots respectively on rough surface and smooth surface are loaded together ( $l(x, y)$  is larger than  $h_0$  at spot  $(x, y)$ ), the gap between them should become zero (contact, positive pressure: domain  $\omega_1$ ), or remain positive (no contact, zero local pressure: domain  $\omega_2$ ). The complementarity problem can be expressed as:

$$h(x, y) = 0, p(x, y) > 0 \quad (x, y) \in \omega_1$$

$$h(x, y) > 0, p(x, y) = 0 \quad (x, y) \in \omega_2$$

$$h(x, y) = h_0 - l(x, y) + \frac{2}{\pi E'} \int_{-\infty}^{+\infty} \int_{-\infty}^{+\infty} \frac{p(x', y') dx' dy'}{\sqrt{(x - x')^2 + (y - y')^2}}$$

In mathematical terms this is a complementarity problem. The two equations are valid on the sub domains  $\omega_1$  and  $\omega_2$  respectively, but the division of the domain  $\omega_1$  and  $\omega_2$  into the two sub domains is a priori unknown. The purpose of this project is to find an efficient and accurate way to solve the above equations by using multigrid method.

### 3. Multigrid Approach

In this project, a multigrid approach is used to solve the above equations and find contact domain, no contact domain and pressure distribution on the surface. First, target grid on the surface is defined as an input of level size (how many grids are discretized on the surface) no matter how many spots on the original input rough surface is. If level size is  $n$ , input surface is discretized into  $2^{n+3}$  grids by  $2^{n+3}$  grids (target grid).

And then beginning with an initial first approximation of the pressure distribution on the surface, the program can calculate the gap between smooth surface and rough surface at contact domain when the pressure of one grid is larger than zero. In above equations, it reflects that the gap in contact zone should be zero, and thus pressure distribution can be adjusted according to the gap between two surfaces. Gap between two surfaces can also be used to check convergence.

In relaxation process, high frequency components are reduced efficiently whereas low frequency components converge only slowly. In that case, starting from an arbitrary first approximation the convergence history will be such that initially a relatively large error reduction may be observed, but after the first few relaxations the convergence speed reduces

to a very slow speed and the error is smooth. One does not need a fine grid to accurately represent it, and thus a full multigrid algorithm is used in this project. Figure 4 shows a full multigrid algorithm 1 V-cycle pre refinement. In order to achieve convergence, in this program number of cycles can be defined by users before running the program. Larger level size needs less number of cycles to achieve convergence.



Figure 4: Full Multigrid Algorithm 1 V-cycle per refinement

## 4. Results

### 4.1. Relation between Contact Pressure and Clearance Height

By using the multigrid approach to solve contact pressure between one rough surface and one smooth surface at clearance height  $h_0$ , relation between contact pressure and clearance height is obtained. The clearance height region between  $2\sigma_p$  to  $4\sigma_p$  ( $\sigma_p$  is plateau surface roughness, calculated by mean square root of plateau) is worth examining because contact between piston ring and liner finish happens in this region in real situations. Figure 5 shows part of the surface geometry of sample liner and relation between contact pressure and lambda ( $\frac{h_0}{\sigma_p}$ ) for this liner finish.

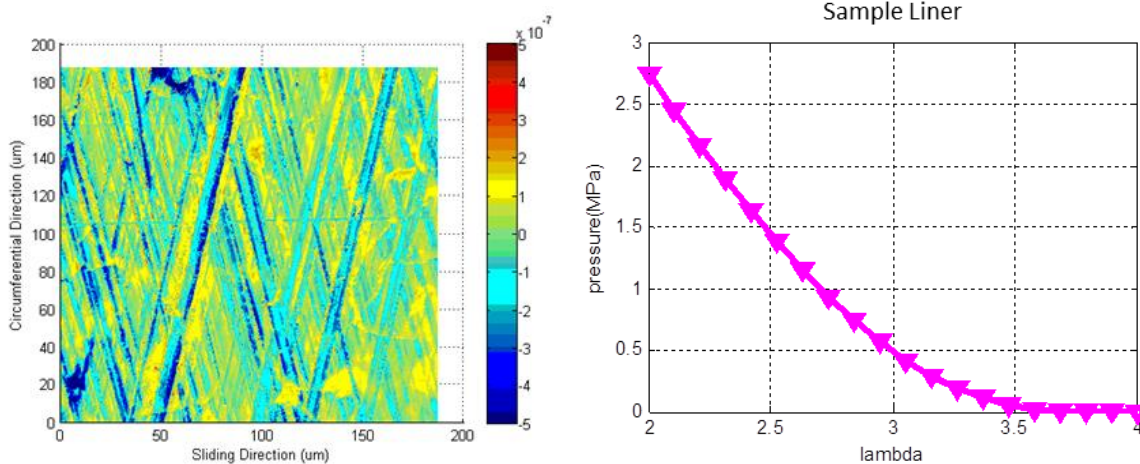
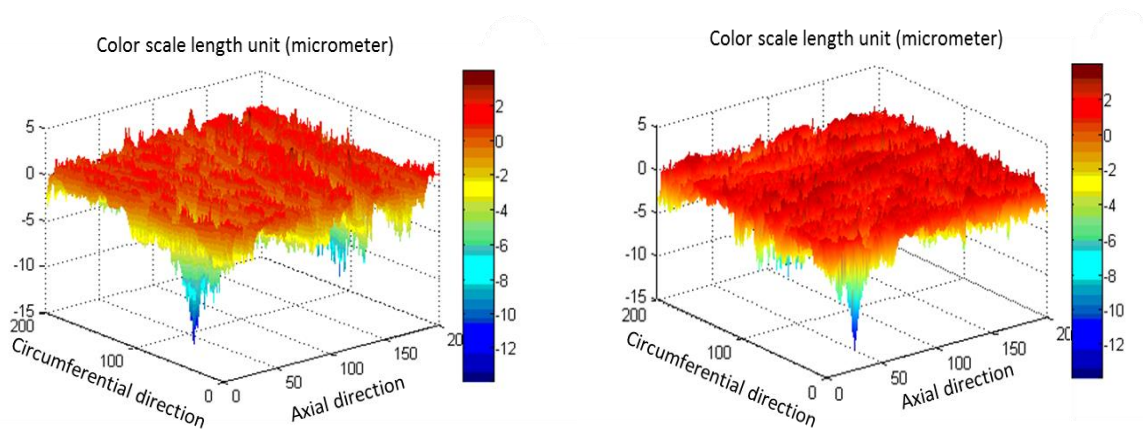


Figure 5: Surface Geometry and Contact Pressure of Sample Liner

#### 4.2. Deformed Rough Surface at Clearance Height

Original measured rough surface and deformed rough surface at clearance height of  $2\sigma_p$  is shown in Figure 6. Large spikes on original rough surface are deformed due to contact with smooth surface and disappear on deformed rough surface. Other areas except large spikes on original surface also deform due to pressure distribution on whole surface, while it is not obvious shown on deformed surface.



**Figure 6: Original Rough Surface and Deformed Rough Surface at  $2\sigma_p$**

#### 4.3. Boundary Effect

In this model, boundary effect has been neglected because input is just the original measured surface and the boundary of rough surface is assumed to be purely smooth and has no contact with smooth surface. However, boundary of rough surface has similar surface geometry as that inside of rough surface and contact pressure at boundary will also deform asperities inside rough surface, and thus boundary effect is not negligible. A surface with center area being real measured rough surface and the outside part being artificially smooth surface is constructed to see the influence of boundary effect, as indicated in Figure 7. Contact pressure on centered rough area of constructed surface neglects boundary effect. The other surface is the real measured liner surface and contact pressure is calculated just in the center part as indicated in Figure 6. This condition considers boundary effect which arises from the outer rough area in the second surface. Contact Pressure on centered part in constructed surface is compared with contact pressure on cycled part in original rough surface, as indicated in Figure 8.

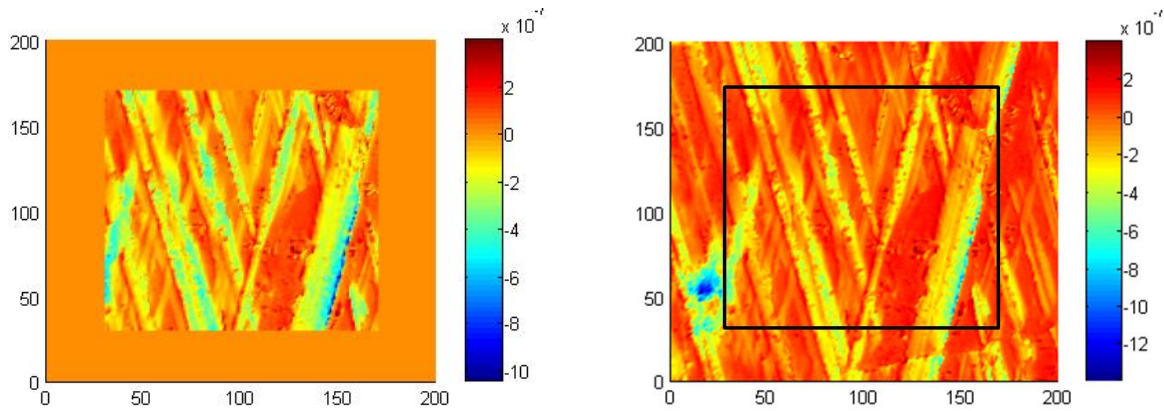


**Figure 7: Constructed Rough Surface without Boundary Effect and Original Rough Surface with Boundary Effect**

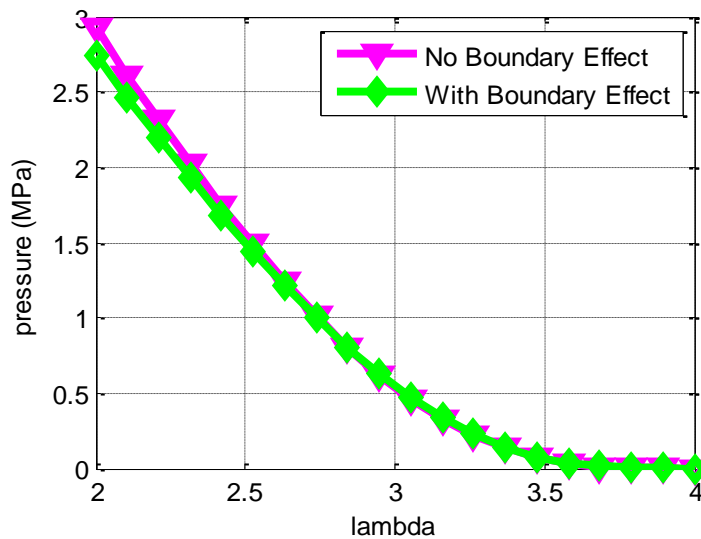


**Figure 8: Comparison of Contact Pressure with Boundary Effect and Contact Pressure without Boundary Effect**

In Figure 8, it indicates that boundary effect in this model is not negligible. Contact pressure due to asperities outside calculation area also deforms asperities inside calculation area and results in smaller contact pressure. By calculating the difference of contact pressure without boundary effect and difference of contact pressure with boundary effect numerically, the maximum difference is around 6 percent which is not small enough to be neglected. In addition, difference depends on area size outside calculation area and it increases with larger area outside calculation area.



#### 4.4. Influence of Level Size

Different level size discretizes rough surface differently. Larger level size gives more grids and smaller grid size, and thus more accurate results. However, it requires more calculation time. Level size 8 which gives 2048 grid by 2048 grid is used to obtain the results shown above in Figure 5 and Figure 8, and this is because there are 3243 grid by 3243 grid on original input surface and level size 8 gives most grids which are less than original grid number on input surface. In order to compare results by different level size, contact pressure of sample liner surface has been calculated at level size 6, level size 7, level size 8 and level size 9 to show the difference, as illustrated in Figure 9, as well as calculation time for each contact pressure, as tabulated in Figure 10.

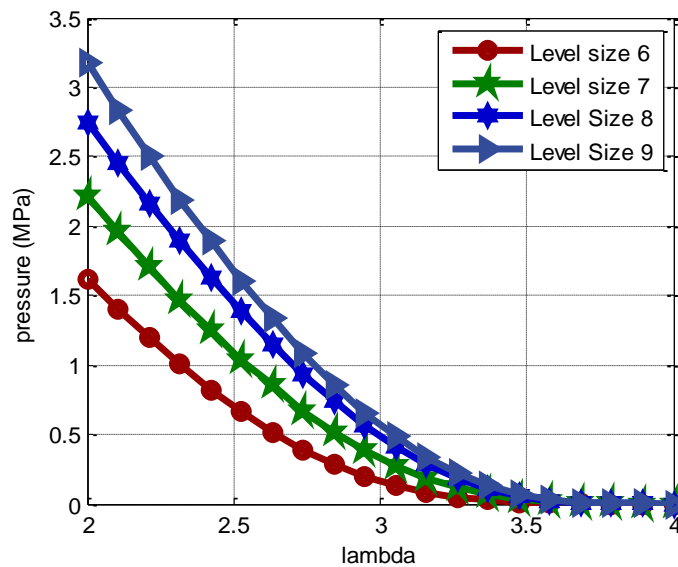


Figure 9: Comparison of Contact Pressure at Different Level Size

	Calculation Time (s)
<b>Compare of Different Level Size</b>	
Level 6	30
Level 7	70
Level 8	300
Level 9	720

Figure 10: Calculation Time at Different Level size



It is found that calculations at level size 6 and level size 7 are inaccurate and predicts less contact pressure than reality. Level size 8 for sample liner is still not enough because there is still a gap between the results at level 8 and level size which is not negligible. Level size 9 is enough for calculation of this sample liner because there are 3243 grid by 3243 grid on the original liner surface and level 9 discretizes the surface into 4096 by 4096 grid.

#### 4.5. Influence of Cycle Number on Convergence

Gap between rough surface and smooth surface at contact domain can serve as a parameter to check residual and convergence speed. In figure 11, it shows normalized residual running under different level size and different number of cycles. At lower level, more cycles are needed to achieve same convergence, but the difference is not large. In this model, normalized residual at the order of  $10^{-4}$  regarded as enough.

Normalized Residual		Number of V cycles										
		3	5	7	8	9	10	11	12	13	14	15
level	Grid Number											
4	N=128	$1.27*10^{-1}$	$4.61*10^{-2}$	$1.72*10^{-2}$	$1.07*10^{-2}$	$6.81*10^{-3}$	$4.35*10^{-3}$	$2.78*10^{-3}$	$1.78*10^{-3}$	$1.14*10^{-3}$	$7.33*10^{-4}$	$4.71*10^{-4}$
5	N=256	$8.29*10^{-2}$	$3.07*10^{-2}$	$1.20*10^{-2}$	$7.55*10^{-3}$	$4.78*10^{-3}$	$3.03*10^{-3}$	$1.93*10^{-3}$	$1.24*10^{-3}$	$7.94*10^{-4}$	$5.10*10^{-4}$	$3.29*10^{-4}$
6	N=512	$6.22*10^{-2}$	$2.26*10^{-2}$	$8.67*10^{-3}$	$5.50*10^{-3}$	$3.48*10^{-3}$	$2.21*10^{-3}$	$1.40*10^{-3}$	$9.00*10^{-4}$	$5.81*10^{-4}$	$3.76*10^{-4}$	$2.44*10^{-4}$
7	N=1024	$4.33*10^{-2}$	$1.54*10^{-2}$	$5.83*10^{-3}$	$3.65*10^{-3}$	$2.31*10^{-3}$	$1.47*10^{-3}$	$9.41*10^{-4}$	$6.06*10^{-4}$	$3.91*10^{-4}$	$2.53*10^{-4}$	$1.65*10^{-4}$
8	N=2048	$2.63*10^{-2}$	$9.41*10^{-3}$	$3.64*10^{-3}$	$2.30*10^{-3}$	$1.46*10^{-3}$	$9.40*10^{-4}$	$6.07*10^{-4}$	$3.93*10^{-4}$	$2.56*10^{-4}$	$1.67*10^{-4}$	$1.09*10^{-4}$
9	N=4096	$1.62*10^{-2}$	$6.00*10^{-3}$	$2.41*10^{-3}$	$1.55*10^{-3}$	$1.01*10^{-3}$	$6.59*10^{-4}$	$4.34*10^{-4}$	$2.87*10^{-4}$	$1.91*10^{-4}$	$1.28*10^{-4}$	$8.55*10^{-5}$

Figure 11: Normalized Residual at Different Level and Different Cycle

#### 4.6. Comparison with Experimental Results

In order to see the practical application of this model, comparisons with experimental results are given. Because in real measurement of friction between liner finish and piston ring pack, measured results are for total friction including contact friction and hydrodynamic friction caused by lubricant between liner finish and piston rings. For prediction, contact comes from this model and hydrodynamic part comes from Tian's cycle model [5].

When piston is at top dead center and bottom dead center in combustion chamber, most of the friction is from contact. Contact dominates when temperature is high and piston speed is slow. In figure 12 and figure 13, total friction between sample liner and oil control ring is compared with experimental data at two different temperatures 40°C and 100°C and 4 different piston speed 100 RPM, 300 RPM, 500 RPM and 700 RPM. The prediction results by this model for

contact friction combined with hydrodynamic friction matches well with experimental data, especially when piston runs at relatively low speed, 100RPM and 300 RPM, it means that contact friction by this model is accurate.

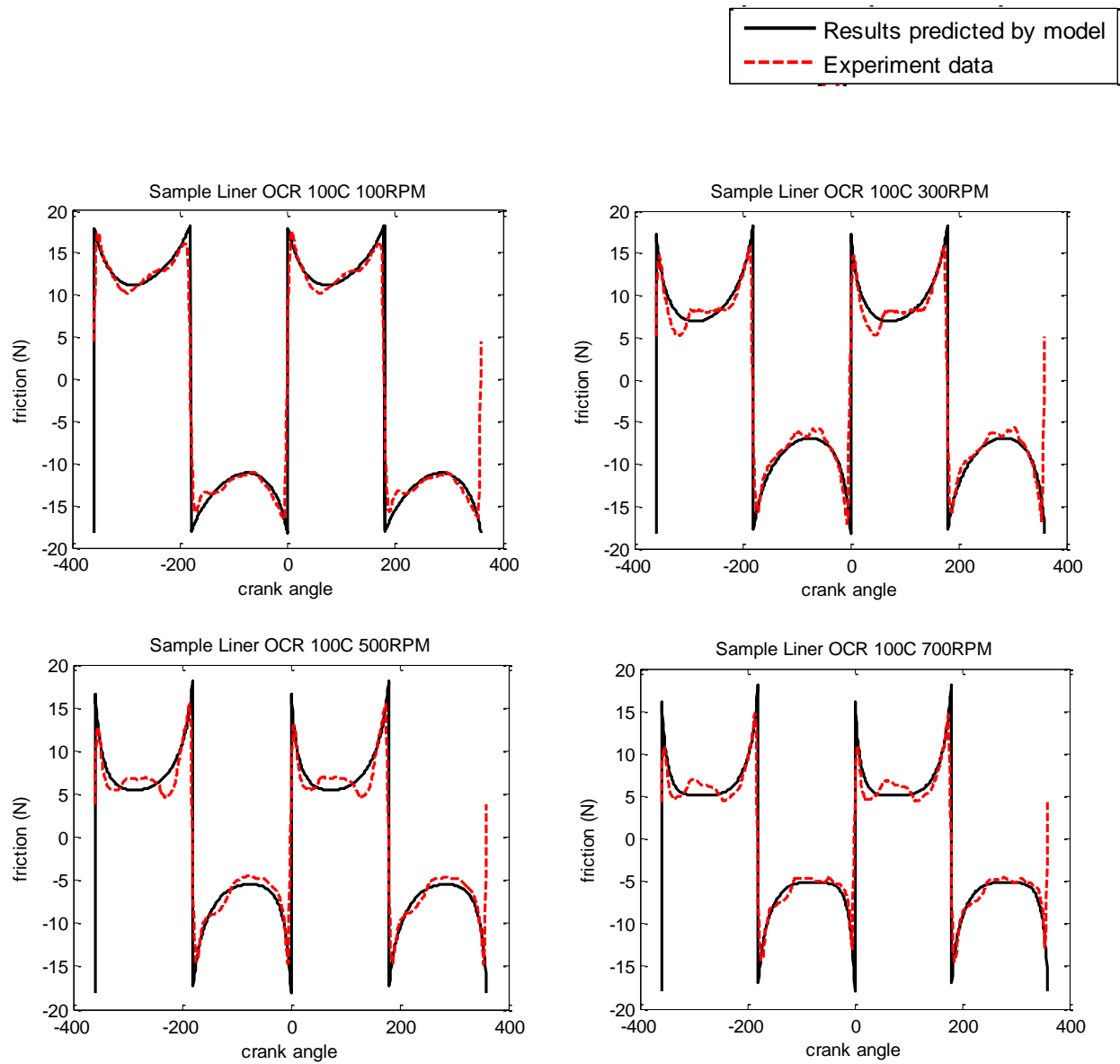


**Figure 12: Comparison of Friction between Sample Liner and Oil Control Ring and Experimental Results at 100°C**

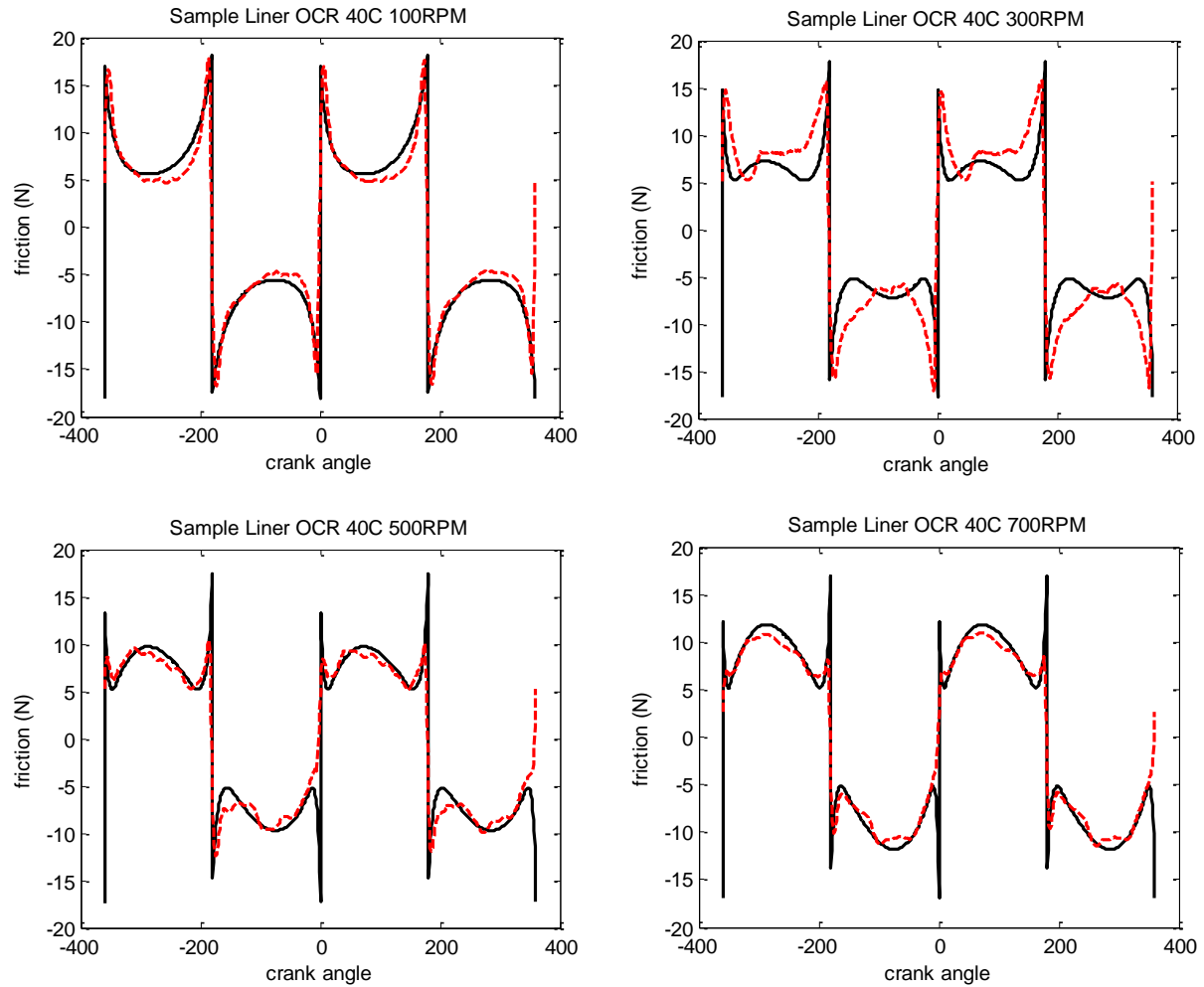


**Figure 12: Comparison of Friction between Sample Liner and Oil Control Ring and Experimental Results at 40°C**

## 5. Conclusion

In this project, a model based on multigrid method is developed to calculate contact pressure between liner finish and piston rings at certain clearance height in internal combustion engines. This model gives meaningful results and match well with experimental data. In addition, this model saves much time by using full multigrid method. In the future, it will serve as a basic model in my research to predict contact between liner finish and piston ring pack. In this work, asperity deformation is only constrained to elastic deformation, but in real conditions plastic deformation exists and should be considered in the future. Additionally, surface geometry evolution will also influence contact and should be considered, especially in break-in process.

**Reference:**

- [1] Richardson, D.E., "Review of Power Cylinder Friction for Diesel Engines", ASME Journal of Engineering for Gas Turbines and Power, 2000, Vol. 122, pp 506-519
- [2] J. Jocsak, V. W. Wong, T. Tian, "The Effects of Cylinder Liner Finish on Piston Ring-Pack Friction", Proceedings of ICEF04, October 2004
- [3] Burscheid, "Piston Ring Handbook", Federal-Mogul Burscheid GmbH, August 2008
- [4] C. H. Venner, A. A. Lubrecht, "Multilevel Methods in Lubrication", Elsevier Science, 2000
- [5] T. Tian, "Modeling the Performance of the Piston Ring-Pack in Internal Combustion Engines", Ph.D. thesis, Department of Mechanical Engineering, MIT, Boston, MA, 1997.